Chiral bands in 135Nd: The interacting boson-fermion model approach

Brant, Slobodan; Petrache, C. M.

Journal article, Published version
Rad u časopisu, Objavljena verzija rada (izdavačev PDF)

Permanent link / Trajna poveznica: https://urn.nsk.hr/urn:nbn:hr:217:506786

Download date / Datum preuzimanja: **2024-06-26**

Repository / Repozitorij:

Repository of the Faculty of Science - University of Zagreb

Chiral bands in ^{135}Nd: The interacting boson-fermion model approach

S. Brant

Department of Physics, Faculty of Science, University of Zagreb, HR-10000 Zagreb, Croatia

C. M. Petrache

Institut de Physique Nucléaire, IN2P3-CNRS and Université Paris-Sud XI, F-91406 Orsay Cedex, France

The chiral interpretation of negative-parity twin bands in the odd-A ^{135}Nd nucleus was investigated in the interacting boson-fermion model. The IBFM calculation shows that the dominant role in the formation of the chiral pattern has the exchange interaction, i.e., the antisymmetrization of odd fermions with the fermion structure of the bosons. The structure of the twin bands in ^{137}Nd has also been investigated, concluding that it is determined by shape fluctuations and prolate-oblate coexistence rather than by chirality.

I. INTRODUCTION

Since the pioneering works of a decade ago [1–3], it has been proposed that the rotation of triaxial nuclei may give rise to pairs of identical $\Delta I = 1$ bands with the same parity in odd-odd nuclei—the chiral doublet bands. The condition for the appearance of chiral doublet bands is that the proton and neutron Fermi levels are located in the lower part of the valence proton high-j (particle-like) and in the upper part of the valence neutron high-j (hole-like) subshells (or vice versa), and the core is triaxial. The angular momenta of the valence particles are aligned along the short and long axes of the triaxial core, while the angular momentum of the rotational core is aligned along the intermediate axis. The three angular momenta can be arranged to form two systems that differ by intrinsic static chirality, a left- and a right-handed system. When this chiral symmetry is broken in the body-fixed frame, the restoration of the symmetry in the laboratory frame results in the occurrence of degenerate doublet $\Delta I = 1$ bands. A number of pairs of bands possibly due to the breaking of the chiral symmetry have been found, and theoretically interpreted, in the $A \sim 105$, $A \sim 130$, and $A \sim 190$ mass regions.

However, the possible formation of chiral bands is not limited to odd-odd nuclei. Whenever three configurations in a nucleus have large angular momentum components along the three principal axes, the conditions for chirality are present. In odd-mass nuclei, this can be fulfilled for three-particle configurations of the type one-proton–two-neutrons or one-neutron–two-protons. In this case, the two-particle configuration takes the role of the one-particle configuration (of the same type) in the odd-odd nucleus. The situation in odd-mass nuclei could be even more favorable for chirality, because the two-particle angular momentum is longer than the one-particle angular momentum in odd-odd nuclei. The proton and neutron configurations are in fact quasiparticle configurations, one being of particle type (occupation probability less than 0.5) and the other of hole type (occupation probability higher than 0.5).

The first observation of a possible three-quasiparticle chiral structure was in ^{135}Nd [4]. The negative-parity ground-state band in ^{135}Nd has the one-neutron-quasiparticle $\nu h_{11/2}$ hole-like structure. In this article, we shall denote this band as band G. At spin 25/2, band G is crossed by a three-quasiparticle band with the structure interpreted by the $\nu h_{11/2}(\pi h_{11/2})^2$ configuration. This band will be denoted as band A. The two-proton-quasiparticle configuration $(\pi h_{11/2})^2$ consists of $\pi h_{11/2}$ particle-like quasiprotons and is therefore particle-like. A twin band interpreted by the same $\nu h_{11/2}(\pi h_{11/2})^2$ configuration, denoted as band B, was observed as the yrare band rather close in excitation energy to band A. In Ref. [4], bands A and B were interpreted as a pair of chiral bands. However, the fact that two bands of the same parity have levels of the same spin close in excitation energy is not a very strong argument to claim that they are chiral bands. To establish whether chirality exists in a certain nucleus, it is crucial to determine the $B(E2)$ and $B(M1)$ values. The electromagnetic transitions deexciting analog states of the chiral twin bands should be almost equal. Recently, $B(E2)$ and $B(M1)$ values deexciting states of bands A and B in ^{135}Nd have been measured [5]. The corresponding $B(E2)$ and $B(M1)$ values have been found to be almost identical in both bands, giving a strong argument for interpreting this pair of bands as chiral partner bands.

The present paper is devoted to the investigation within the interacting boson-fermion plus broken pairs framework [6] of the properties of the three-quasiparticle bands in ^{135}Nd and in the $N = 77$ neighboring nucleus ^{137}Nd.

II. IBFM CALCULATIONS

In a number of articles, several theoretical models, such as the tilted axis cranking model [1], two quasiparticle + triaxial rotor model [1,7], and core-particle-hole coupling model [8], have been applied in the interpretation of chiral bands in odd-odd nuclei. Calculations in the interacting boson-fermion-fermion model (IBFFM-1) [9,10], in the version where there is no distinction between proton bosons and neutron bosons, have been performed for ^{134}Pr [11–13]. The IBFFM-1 is based on the interacting boson model (IBM-1) [14,15] for even-even

nuclei, and the interacting boson-fermion model (IBFM-1) [16,17] for odd-A nuclei. The standard boson Hamiltonian of the IBM-1, with up to two-body boson interactions,

$$H_B = \epsilon \, \hat{N} + \frac{1}{2} \, V_0([d^\dagger d^\dagger]_0 \, [\tilde{s}\tilde{s}]_0 + \text{h.c.})_0$$
$$+ \frac{1}{\sqrt{2}} \, V_2([d^\dagger d^\dagger]_2 [\tilde{d}\tilde{s}]_2 + \text{h.c.})_0$$
$$+ \sum_{L=0,2,4} \frac{1}{2} \, C_L \sqrt{2L+1} \, ([d^\dagger d^\dagger]_L [\tilde{d}\tilde{d}]_L)_0, \quad (1)$$

can describe nuclei with spherical, axial, γ-unstable, and transitional shapes. In the O(6) limit, triaxiality reduces to γ instability for finite boson systems. The potential energy surface is flat in the γ direction but is also rather broad in the β direction, and the effective γ_{eff} is $30°$. With the addition of a cubic (three-body) term [18,19]

$$H_{\text{cub}} = \Theta_3([d^\dagger d^\dagger]_2 \, d^\dagger)_3 \cdot ([\tilde{d} \, \tilde{d}]_2 \tilde{d})_3 \quad (2)$$

to the standard IBM-1 Hamiltonian, a triaxial equilibrium deformation is generated, but the minimum is still broad [18] and the fluctuations of the shape large. Since all odd-odd nuclei in which chiral bands have been observed are in regions of masses where even-even nuclei are γ-soft, i.e., effectively triaxial but not rigid, the application of models based on the interacting boson approximation in the description of chiral bands can be successful. The conclusion in Refs. [12,13] was that in ^{134}Pr, the possibility for angular momenta of the valence proton, neutron, and core to find themselves in the favorable, almost orthogonal geometry is present, but not dominant. Shape fluctuations are found to be rather large, and the chirality weak and of dynamical origin. The analysis in IBFFM-1 of the structure of odd-odd nuclei where both the level energies and the electromagnetic decay properties display the chiral pattern, and of those where a pair of twin bands is only close in excitation energy, has shown that the difference in the structure of the two types of chiral candidate nuclei can be attributed to different β and γ fluctuations, induced by the exchange boson-fermion interaction of the interacting boson-fermion-fermion model [20]. The effect of the Pauli principle, contained in the exchange boson-fermion interaction, seems to play a dominant role.

Models based on the interacting boson approximation can be extended for a description of high-spin states in even-even [21] and odd-even [6] nuclei. The model space is extended by including part of the original shell-model fermion space through successive breaking of correlated S and D pairs (s and d bosons). In even-even nuclei, high-spin states are generated not only by the alignment of d bosons, but also by coupling fermion pairs to the boson core. A boson can be destroyed, i.e., a correlated fermion pair can be broken by the Coriolis interaction, and the resulting noncollective fermion pair recouples to the core. The structure of high-spin states is therefore determined by broken pairs. In odd-even nuclei, the basis consists of one-fermion and three-fermion configurations. The two fermions in the broken pair can be of the same type as the unpaired fermion, resulting in a space with three identical fermions. If the fermions in the broken pair are different from the unpaired one, the fermion basis contains two

protons and one neutron or vice versa. For odd-mass nuclei, the model is called the interacting boson-fermion plus broken pairs model (IBFBPM). For simplicity, in this article we will use the name IBFM. This model was also applied in the description of even-even and odd-even nuclei in the Nd-Sm region [22–25].

In this article, negative-parity bands in ^{135}Nd are described in the framework of the interacting boson-fermion plus broken pairs model with the Hamiltonian

$$H = H_B + H_{\text{cub}} + H_{\nu F} + H_{\pi F}$$
$$+ V_\pi^{\text{mix}} + V_{\nu\pi} + V_{\nu BF} + V_{\pi BF}. \quad (3)$$

$H_{\nu F}$ is the single-fermion (neutron) Hamiltonian which contains neutron quasiparticle energies

$$H_{\nu F} = \sum_i \varepsilon_{\nu_i} \, a_{\nu_i}^\dagger \tilde{a}_{\nu_i}, \quad (4)$$

while $H_{\pi F}$ in addition contains the proton-proton interaction

$$H_{\pi F} = \sum_i \varepsilon_{\pi_i} \, a_{\pi_i}^\dagger \tilde{a}_{\pi_i}$$
$$+ \frac{1}{4} \sum_{abcd} \sum_{JM} V_{\pi abcd}^J \, A_{JM}^\dagger(\pi_a \pi_b) \, A_{JM}(\pi_c \pi_d), \quad (5)$$

where the proton pair operator is defined as

$$A_{JM}^\dagger(\pi_a \pi_b) = \frac{1}{\sqrt{1+\delta_{ab}}} [a_{\pi_a}^\dagger \, a_{\pi_b}^\dagger]_J^M. \quad (6)$$

The proton pair breaking interaction V_π^{mix} is

$$V_\pi^{\text{mix}} = -U_2 \sum_{\pi j_1 \pi j_2} (u_{\pi j_1} v_{\pi j_2} + u_{\pi j_2} v_{\pi j_1}) \langle \pi j_1 \parallel Y_2 \parallel \pi j_2 \rangle$$
$$\times ([a_{\pi j_1}^\dagger a_{\pi j_2}^\dagger]_2 \cdot \tilde{d}) + \text{h.c.} \quad (7)$$

The proton-neutron interaction is

$$V_{\nu\pi} = \sum_{\nu\nu'\pi\pi'} \sum_J h_J(\nu\nu'\pi\pi')(u_\nu u_{\nu'} - v_\nu v_{\nu'})$$
$$\times (u_\pi u_{\pi'} - v_\pi v_{\pi'})([a_\nu^\dagger \tilde{a}_{\nu'}]_J \cdot [a_\pi^\dagger \tilde{a}_{\pi'}]_J), \quad (8)$$

where the coefficients $h_J(\nu\nu'\pi\pi')$ are connected to the two-body matrix elements of the residual proton-neutron interaction by

$$h_J(\nu\nu'\pi'\pi) = (-)^{j_\nu + j_\pi} \sum_{J'} (-)^{J'} \sqrt{2J'+1}$$
$$\times \langle (j_\nu j_\pi)J' \parallel V(1,2) \parallel (j_{\nu'} j_{\pi'})J' \rangle$$
$$\times W(j_\nu j_\pi j_{\nu'} j_{\pi'}; J'J). \quad (9)$$

$V_{\nu BF}$ and $V_{\pi BF}$ are the IBFM-1 boson-fermion (neutron) and boson-fermion (proton) interactions containing the dynamical (direct), exchange, and the less important monopole term

$$V_{BF} = V_{\text{dyn}} + V_{\text{exc}} + V_{\text{mon}}, \quad (10)$$

where

$$V_{\text{dyn}} = \Gamma_0 \sum_{j_1 j_2} \sqrt{5} \, (u_{j_1} u_{j_2} - v_{j_1} v_{j_2}) \langle j_1 \parallel Y_2 \parallel j_2 \rangle$$
$$\times ([a_{j_1}^\dagger \tilde{a}_{j_2}]_2 \, Q_2^B)_0, \quad (11)$$

where Q_2^B is the boson quadrupole operator

$$Q_2^B = [s^\dagger \tilde{d} + d^\dagger \tilde{s}]_2 + \chi [d^\dagger \tilde{d}]_2 + \eta([d^\dagger \tilde{d}]_3 [d^\dagger \tilde{d}]_3)_2, \quad (12)$$

$$V_{\mathrm{exc}} = \Lambda_0 \sum_{j_1 j_2 j_3} (-2) \sqrt{\frac{5}{2j_3 + 1}} \, (u_{j_1} v_{j_3} + v_{j_1} u_{j_3})$$
$$\times (u_{j_2} v_{j_3} + v_{j_2} u_{j_3}) \langle j_3 \parallel Y_2 \parallel j_1 \rangle \langle j_3 \parallel Y_2 \parallel j_2 \rangle$$
$$: ([a_{j_1}^\dagger \tilde{d}]_{j_3} [\tilde{a}_{j_2} d^\dagger]_{j_3})_0 :, \quad (13)$$

$$V_{\mathrm{mon}} = A_0 \sum_j \sqrt{5} \, (2j+1)([a_j^\dagger \tilde{a}_j]_0 [d^\dagger \tilde{d}]_0)_0. \quad (14)$$

The configuration independent strengths of the boson-fermion interactions Γ_0, Λ_0, and A_0 in Eqs. (11), (13), and (14) we denote as Γ_0^ν, Λ_0^ν, A_0^ν or Γ_0^π, Λ_0^π, A_0^π for $V_{\nu BF}$ and $V_{\pi BF}$, respectively. The occupation probabilities, fermion angular momenta, and fermion operators are for neutrons or protons respectively, too.

For the core nucleus ^{136}Nd, the set of parameters for the IBM-1 boson Hamiltonian [14] is (all values in MeV): $\epsilon = 0.12$, $V_0 = -0.24$, $V_2 = 0.01$, $C_0 = 0.16$, $C_2 = 0.06$, $C_4 = 0.19$. The number of bosons N in the IBM scheme is equal to half the number of valence nucleon particles and holes. For ^{136}Nd, $N = 8$. The IBM-1 parametrization for ^{136}Nd, adopted in this article, gives the structure of ^{136}Nd that basically differs from the one in Ref. [25] only in the excitation energies of the 0_2^+ and related levels. For the present parametrization, the excitation energy of the 0_2^+ level is 0.54 MeV higher than it was assumed in Ref. [25]. The excitation energy of the 0_2^+ level in ^{136}Nd is not known, but the level systematics in this region suggests that is higher than predicted in Ref. [25]. Nevertheless, levels that belong to the band structure associated with the 0_2^+ state do not contribute in the structure of high-spin states. The strength of the cubic (three-body) term is $\Theta_3 = 0.017$ MeV. The structure of ^{136}Nd in IBM-1 is very similar to the structure of ^{134}Ce, the core nucleus for ^{134}Pr [11–13]. It is γ-soft with a triaxial equilibrium deformation, but the minimum is broad, and the fluctuations of the shape large.

For the neutrons, the single-particle energies, except for the shifts of orbitals from the $N = 82$–126 shell, are taken from the calculations for ^{134}Pr [11–13]: 0, 0.4, 1.6, 2.0, 2.3, 7.6, 9.3, and 9.4 (all values in MeV), for $\nu d_{5/2}$, $\nu g_{7/2}$, $\nu s_{1/2}$, $\nu d_{3/2}$, $\nu h_{11/2}$, $\nu f_{7/2}$, $\nu p_{3/2}$, and $\nu h_{9/2}$, respectively. Calculations for ^{138}Nd [23] have shown that the excitation energy of the 10^+ $(\nu h_{11/2})^2$ level requires the quasiparticle energy of the $\nu h_{11/2}$ configuration of 1.6 MeV. Being the quasiparticle energies of the $\nu h_{11/2}$ configuration 1.65 MeV in ^{137}Nd [24] and ^{139}Sm [22], we should expect 1.70 MeV in ^{135}Nd, which is obtained by employing the pairing strength $G = 29/A$ MeV, which is bigger than the standard value $G = 23/A$ MeV. From a BCS calculation with the pairing strength $G = 29/A$ MeV, the $\nu h_{11/2}$, $\nu f_{7/2}$, and $\nu p_{3/2}$ quasiparticles, with the resulting quasiparticle energies ε and occupation probabilities ν^2, $\varepsilon(\nu h_{11/2}) = 1.70$ MeV, $\varepsilon(\nu f_{7/2}) = 5.16$ MeV, $\varepsilon(\nu p_{3/2}) = 6.80$ MeV, $\nu^2(\nu h_{11/2}) = 0.62$, $\nu^2(\nu f_{7/2}) = 0.02$, and $\nu^2(\nu p_{3/2}) = 0.01$, are included in the fermion basis. For the boson-fermion interaction strengths

for neutrons, we take $\Gamma_0^\nu = 0.7$, $\Lambda_0^\nu = 1.4$, $A_0^\nu = 0.1$ (all values in MeV) in the space of one-quasiparticle configurations, and $\Gamma_0^\nu = 0.5$, $\Lambda_0^\nu = 1.9$, $A_0^\nu = 0.07$ (all values in MeV) in the space of three-quasiparticle configurations. The interaction strengths are in the range of strengths that generate chiral bands in odd-odd nuclei [12,13,20]. The parameters $\chi = -0.6$ and $\eta = -0.35$ (defined in Ref. [11]) in the quadrupole operator of the dynamical boson-fermion interaction are same as in Refs. [12,13,20].

The proton quasiparticle energies and occupation probabilities are obtained by a BCS calculation with the following single-particle energies: 0.18, 0.795, 2.248, 3.2, 3.41, 6.0, 6.5 MeV, for $\pi g_{7/2}$, $\pi d_{5/2}$, $\pi h_{11/2}$, $\pi d_{3/2}$, $\pi s_{1/2}$, $\pi h_{9/2}$, $\pi f_{7/2}$, respectively, and with the pairing strength $G = 23/A$ MeV. The same single-particle energies and pairing strength have been used in the calculations for ^{134}Pr [11–13]. In the basis for the ^{135}Nd calculations, $\pi h_{11/2}$ and $\pi f_{7/2}$ proton quasiparticles are included with quasiparticle energies and occupation probabilities: $\varepsilon(\pi h_{11/2}) = 1.91$ MeV, $\varepsilon(\pi f_{7/2}) = 5.91$ MeV, $\nu^2(\pi h_{11/2}) = 0.09$, and $\nu^2(\pi f_{7/2}) = 0.01$. Since due to the spin-flip matrix element $\langle \pi h_{11/2} || Y_2 || \pi h_{9/2} \rangle \pi h_{9/2}$ components are not admixed into the wave functions based on the $\pi h_{11/2}$ configuration, the $\pi h_{9/2}$ quasiparticle is not included in the basis. From the calculation of negative-parity states in the odd-Z neighbor $^{137}_{61}$Pm$_{76}$, the boson-fermion interaction strengths for protons are deduced: $\Gamma_0^\pi = 0.32$, $\Lambda_0^\pi = 0.5$, $A_0^\pi = 0.03$ (all values in MeV). The parameters $\chi = -0.6$ and $\eta = -0.35$ in the quadrupole operator of the dynamical boson-fermion interaction are the same as for neutrons. The parametrization for protons differs only in details from the parametrization used for ^{134}Pr. Odd-Z nuclei in this region have a very similar decoupled structure of one-quasiproton negative-parity states.

The strength parameter of the proton pair-breaking interaction $U_2 = 0.2$ MeV is taken the same as in ^{137}Nd [24]. Although the calculations have shown that the residual interaction between unpaired protons does not influence the structure of the chiral candidate bands A and B, for completeness it was taken as the volume δ-interaction $V_{\pi\pi'} = 4\pi V_{\delta\pi\pi'} \delta(\mathbf{r}_\pi - \mathbf{r}_{\pi'})$ with the strength $V_{\delta\pi\pi'} = -10.0$ MeV. This strength gives the values of matrix elements similar as the surface δ-interaction with the strength -0.1 MeV in ^{137}Nd [24]. The residual proton-neutron interaction is taken as a tensor interaction $V(1, 2) = V_T V(r)[3(\sigma_\pi \cdot \mathbf{r}_{\pi\nu})(\sigma_\nu \cdot \mathbf{r}_{\pi\nu})/\mathbf{r}_{\pi\nu}^2 - (\sigma_\pi \cdot \sigma_\nu)]$ with the Gaussian radial dependence $V(r) = \exp(-r^2/r_0^2)$ with the strength $V_T - 14.5$ MeV and range $r_0 = 2.7$ fm [20]. For the tensor interaction, the BCS dependent terms in Eq. (8) contain the sum instead of the difference of BCS amplitudes.

In the calculation of $B(E2)$ and $B(M1)$ values, we use the effective charges and gyromagnetic ratios: $e^\pi = 1.0$, $e^\nu = 0.5$, $e^{\mathrm{vib}} = 1.3$, $g_l^\pi = 1$, $g_s^\pi = 0.9 g_s^{\pi,\mathrm{free}} = 5.027$, $g_l^\nu = 0$, $g_s^\nu = 0.5 g_s^{\nu,\mathrm{free}} = -1.913$, and $g_R = 0.6$. The parameters $\chi = -0.6$ and $\eta = -0.35$ in the boson quadrupole operator have the same values as in the quadrupole operators of the dynamical boson-fermion interactions. Except for e^{vib}, g_s^π, and g_R, the effective charges and gyromagnetic ratios are the same as in calculations for ^{134}Pr. The value of g_s^π is close to $g_s^\pi = g_s^{\pi,\mathrm{free}} = 5.586$ in ^{137}Nd. The boson charge e^{vib} is adjusted to
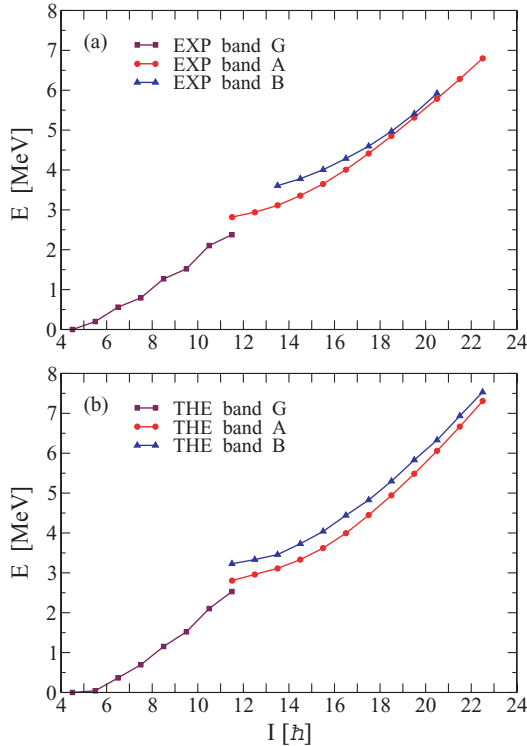
FIG. 1. (Color online) (a) Experimental and (b) calculated negative-parity structure in ^{135}Nd. The $\nu h_{11/2}$ ground-state band is denoted as band G. The pair of twin bands based on $\nu h_{11/2}(\pi h_{11/2})^2$ configuration are denoted as band A and band B.
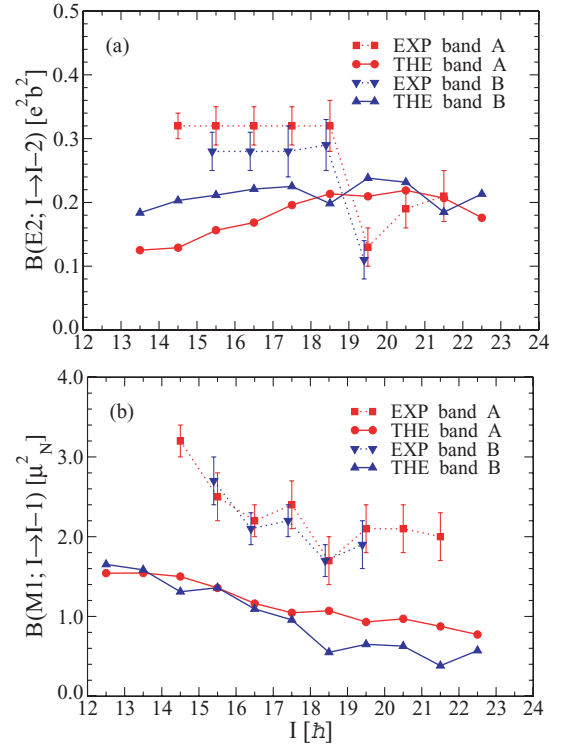

FIG. 2. (Color online) Experimental (EXP) and calculated (THE) $B(E2)$ and $B(M1)$ values for transitions in the yrast band A and side band B in ^{135}Nd. (a) $B(E2)$ values. (b) $B(M1)$ values for $\Delta I = 1$ transitions.

reproduce the $B(E2)(2_1^+ \rightarrow 0_1^+)$ experimental value in ^{136}Nd and is only slightly bigger than $e^{\mathrm{vib}} = 1.2$ in ^{134}Pr.

In Fig. 1, calculated excitation energies in the negative-parity bands G, A, and B in ^{135}Nd are shown in comparison with the experimental data. The comparison of calculated $B(E2)$ and $B(M1)$ values for transitions in the yrast band A and side band B with the experimental data is presented in Fig. 2.

III. DISCUSSION

The calculated negative-parity ground-state band G, as expected, has the one-neutron-quasiparticle $\nu h_{11/2}$ structure up to spin 23/2. States of this band with higher spins are above the states of the three-quasiparticle bands. At spin 25/2, the calculated band A with the structure $\nu h_{11/2}(\pi h_{11/2})^2$ becomes the yrast band. A twin band B, with the same $\nu h_{11/2}(\pi h_{11/2})^2$ configuration and rather close in excitation energy to band A, becomes the yrare band.

The result of the IBFM calculations is that both bands, A and B, are basically built on the ground-state band of the even-even core. The admixture of the γ-band components of the core is small. With increasing angular momentum, the admixture of the γ-band components of the core becomes smaller. For states with spins 23/2–35/2, the percentage of γ-band components in the wave functions amounts to 15–20%. For states with spins 37/2 and 39/2, it gradually decreases; and for states with spins 41/2–45/2, the percentage of γ-band

components is stable around 10%. This behavior is different from that in the IBFFM wave functions of odd-odd nuclei. The two-proton angular momentum is twice as long as the one-proton angular momentum in the neighboring odd-odd nuclei, providing a better possibility for the formation of chiral structures.

The geometrical picture can be revealed in the analysis of the distributions $\zeta(J_\pi j_\nu)$, $\psi(J_\pi R)$, and $\xi(j_\nu R)$ of the angles between $\mathbf{J}_\pi$, $\mathbf{j}_\nu$, and $\mathbf{R}$, of the σ distribution, and of the distribution of the instantaneous values of the β and γ deformation parameters (details of the procedure can be found in Ref. [13], where instead, for the two-proton angular momentum $\mathbf{J}_\pi$, the angles are defined for the one-proton angular momentum $\mathbf{j}_\pi$). This analysis shows that in the states of bands A and B, the presence of configurations with the angular momenta of the protons, neutron, and core is substantial in the chirality-favorable, almost orthogonal geometry. It is not as pronounced as if it were for a rigid triaxial core, but it is far more pronounced than in the case of neighboring odd-odd nuclei [13,20]. The comparisons of the calculated ζ, ψ, ξ, and σ distributions for the $I = 39/2$ yrast and yrare states in ^{135}Nd and for the $I = 15$ yrast and yrare states in ^{134}Pr [13] are presented in Figs. 3 and 4. The states are chosen such that they have eight units of angular momentum more than the corresponding bandheads, i.e., four units of angular momentum more than the corresponding maximal fermion alignments. The orientation of $\mathbf{J}_\pi$, $\mathbf{j}_\nu$ and $\mathbf{R}$ in analog states of the twin bands A and B in ^{135}Nd is very similar. The

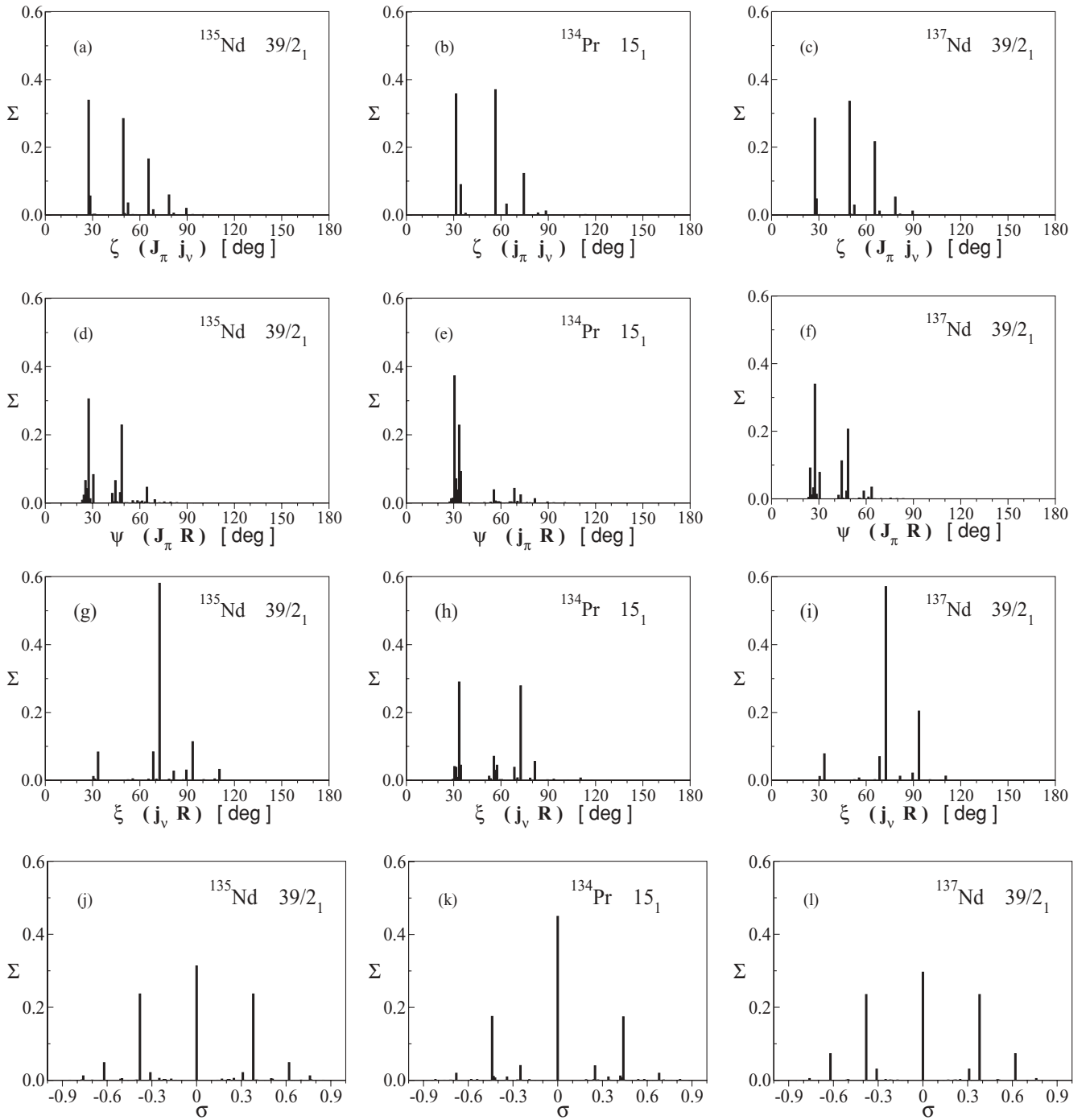FIG. 3. Calculated distributions (a) $\zeta\,(J_\pi\,j_\nu)$, (d) $\psi\,(J_\pi\,R)$, and (g) $\xi\,(j_\nu\,R)$ of the angles between $\mathbf{J}_\pi$, $\mathbf{j}_\nu$, and $\mathbf{R}$, and (j) the σ distribution for the $39/2_1$ state of the yrast band A in ^{135}Nd. Panels (b), (e), (h), and (k) present the corresponding distributions for the yrast $\pi h_{11/2}\,\nu h_{11/2}$ 15_1 state in ^{134}Pr. Panels (c), (f), (i), and (l) show the corresponding distributions for the $39/2_1$ state of the yrast band A in ^{137}Nd.

$\zeta\,(J_\pi\,j_\nu)$, $\psi\,(J_\pi\,R)$, $\xi\,(j_\nu\,R)$ and σ distributions do not show dramatic changes in the patterns for medium- and high-spin states of bands A and B, especially not such that could generate sizable changes in the electromagnetic decay patterns. The structural change in bands A and B is a consequence of shape fluctuations (Fig. 5). For states with $I \leqslant 35/2$, shape fluctuations are of the order of those in the neighboring odd-odd nuclei [13,20]. At spin 37/2, shape fluctuations are

reduced; and for higher spins, although different values of β are present, the distribution shows one dominant peak. The structure changes from the geometry dominated by shape fluctuations into the geometry that is rather close to static chirality. The transition from the vibrational into a static chiral regime of bands A and B has recently been obtained in the calculations of tilted axis cranking (TAC) model with the random-phase approximation (RPA) [5].
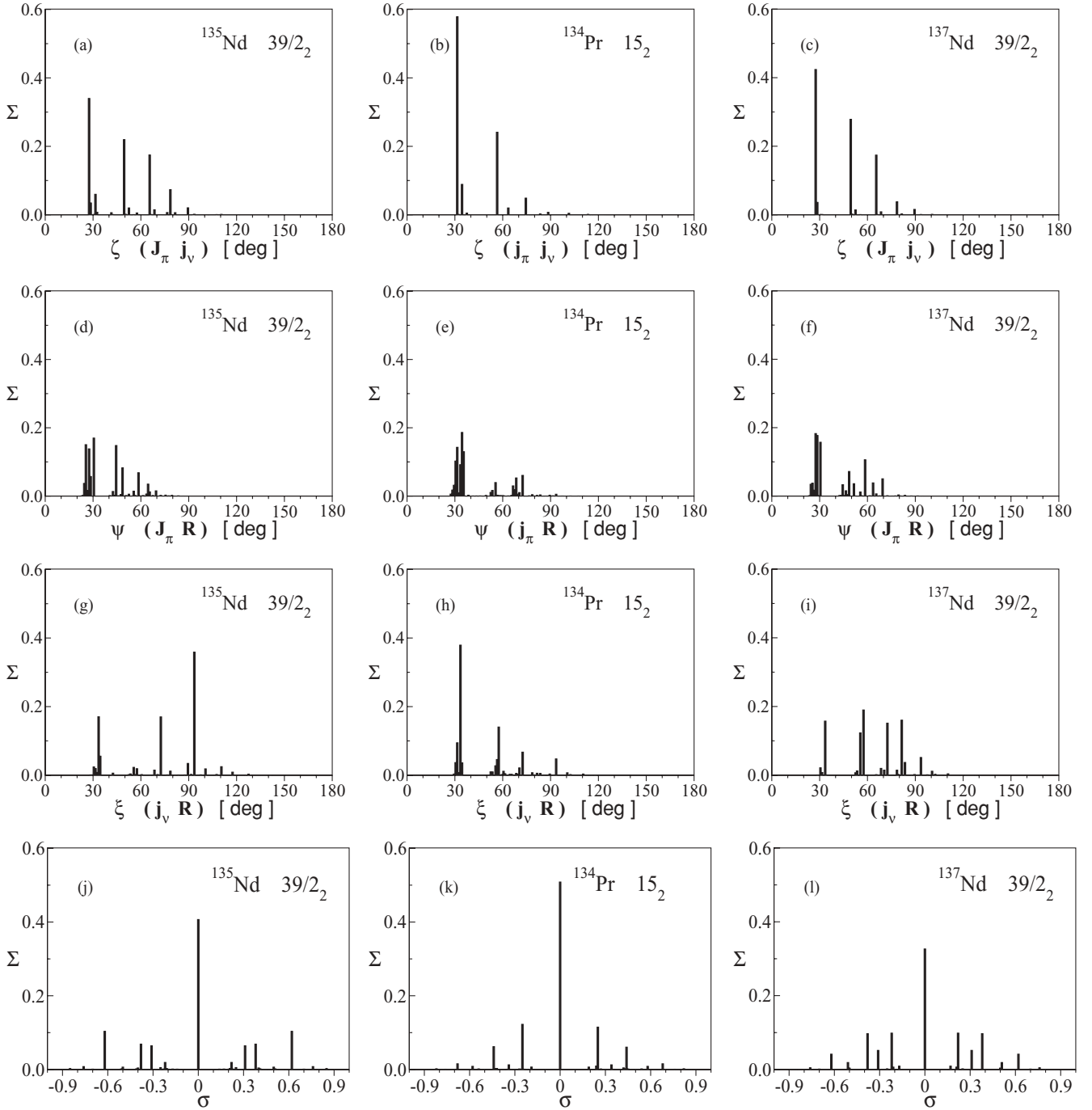
FIG. 4. Calculated distributions (a) ζ $(J_\pi\, j_\nu)$, (d) ψ $(J_\pi\, R)$, and (g) ξ $(j_\nu\, R)$ of the angles between $\mathbf{J}_\pi$, $\mathbf{j}_\nu$, and $\mathbf{R}$, and (j) the σ distribution for the $39/2_2$ state of the yrare band B in ^{135}Nd. Panels (b), (e), (h), and (k) present the corresponding distributions for the yrare $\pi h_{11/2}\, \nu h_{11/2}$ 15_2 state in ^{134}Pr. Panels (c), (f), (i), and (l) show the corresponding distributions for the $39/2_2$ state of the yrare band B in ^{137}Nd.

Except for states with spins 23/2–27/2, where the two-quasiproton configuration in the wave functions is a combination of $[(\pi h_{11/2})^2]8$ and $[(\pi h_{11/2})^2]10$ components, all other states in bands A and B have the proton structure $[(\pi h_{11/2})^2]10$. In fact, bands A and B are formed by a coupling of the $\nu h_{11/2}$ quasiparticle to the band with a bandhead 10^+, based on the quasiproton $[(\pi h_{11/2})^2]10$ configuration in the core ^{136}Nd nucleus [25].

The calculated $B(E2)$ values for transitions deexciting partner states of bands A and B differ by a factor of 1.3–1.5 for the lowest states. Starting from spin 35/2 they are almost equal. At spin 37/2 a drop in the $B(E2)$ is predicted, followed by a rise of the $B(E2)$ values. The same effect is predicted in the framework of TAC complemented by RPA calculations and confirmed by experimental data [5], except that in IBFM it is not so pronounced and appears at spin 37/2 only in band
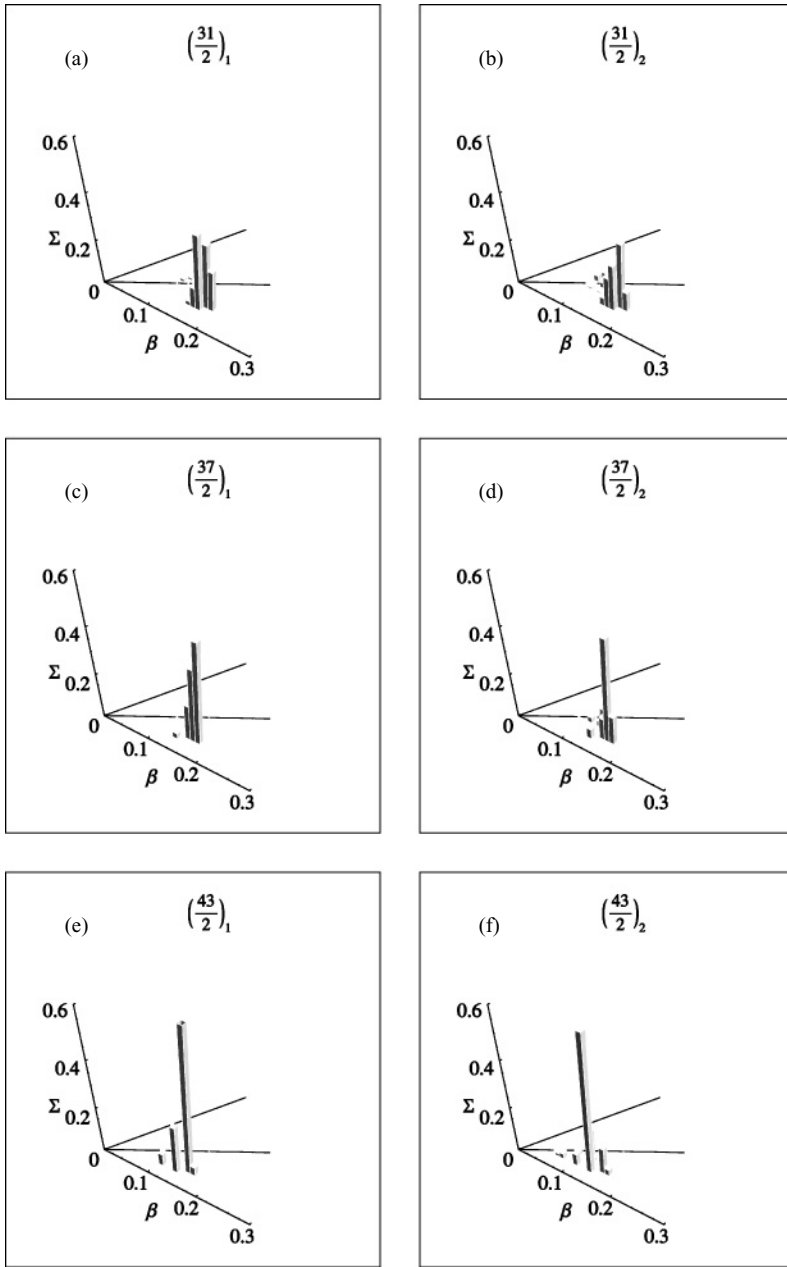
FIG. 5. IBFM β and γ distributions in ^{135}Nd, defined as in Ref. [13], for the (a) $31/2_1$ and (b) $31/2_2$ states; the (c) $37/2_1$ and (d) $37/2_2$ states; and the (e) $43/2_1$ and (f) $43/2_2$ states. The axes in the β-γ plane have $\gamma = 0°$ and $\gamma = 60°$, while the middle line in the β-γ plane marks $\gamma = 30°$.

B. Due to the truncation of the boson space in IBM, states at the top of the bands lose collectivity, and the expected rise in $B(E2)$ values cannot be obtained. The calculated interband $B(E2)$ values are much smaller than the observed ones. The same are the predictions in Ref. [5], but the interband $B(E2)$ values in IBFM are smaller than in TAC/RPA.

The calculated $B(M1)$ values for transitions deexciting partner states of bands A and B are almost equal up to spin 35/2 in both bands, followed by a drop at spin 37/2 in band B and by moderately stronger $B(M1)$ values in band A for higher states. The functional form is similar to the experimental and theoretical in Ref. [5]. The same are the predictions for the interband $B(M1)$ values, which similarly to those calculated in Ref. [5] are smaller than the experimental.

The present IBFM calculation, as well as the calculation in the TAC/RPA framework, gives smaller theoretical than observed $B(E2)$ and $B(M1)$ values (in IBFM on average by a factor 2), the TAC/RPA values being closer to the observed ones. In IBFM, the values of effective charges and gyromagnetic ratios are taken close to the values previously used in a number of articles in this region. For the magnitude of $B(E2)$ values, the value of the boson charge e^{vib} is critical. As already stated, it is adjusted to reproduce the $B(E2)(2_1^+ \rightarrow 0_1^+)$ experimental value in ^{136}Nd, giving the calculated value of the quadrupole moment of the 9/2 state in ^{135}Nd, $Q(9/2) = +1.18\,e$ b (the observed value is $Q(9/2) = +1.9\,(5)\,e$ b). For the present choice of gyromagnetic ratios, the observed values of the magnetic moments of the 9/2 and 11/2 states, $\mu(9/2) = -0.78\,(3)\,\mu_N$ and $\mu(11/2) = -0.50\,(31)\,\mu_N$ are reproduced
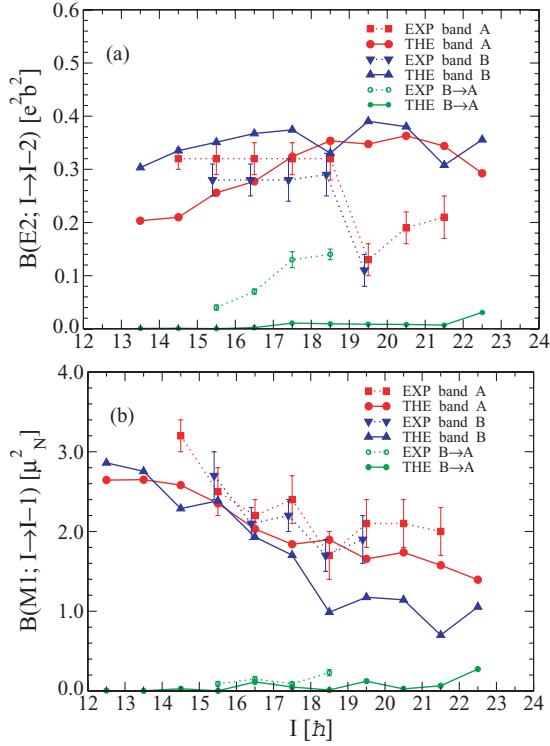
FIG. 6. (Color online) Experimental (EXP) and calculated (THE) $B(E2)$ and $B(M1)$ values in ^{135}Nd for intraband transitions in the yrast band A and side band B, and for the interband transitions deexciting states in band B. (a) $B(E2)$ values. (b) $B(M1)$ values for $\Delta I = 1$ transitions. The $B(E2)$ values are calculated with $e^{\mathrm{vib}} = 1.7$. For the $B(M1)$ values, the fermion gyromagnetic ratios are $g_l^\pi = 1.1$, $g_s^\pi = g_s^{\pi,\mathrm{free}} = 5.586$, $g_l^\nu = -0.1$, and $g_s^\nu = g_s^{\nu,\mathrm{free}} = -3.826$. The remaining charges and gyromagnetic ratios are the same as in the parametrization adopted in Fig. 2.

well. The calculated values are $\mu(9/2) = -0.89\,\mu_N$ and $\mu(11/2) = -0.59\,\mu_N$.

Since the core ^{136}Nd nucleus is γ-soft, the alignment of specific quasiparticle pairs not only can readily change the nuclear shape, but also could possibly influence the renormalization of effective charges and gyromagnetic ratios. For comparison, assuming that there is not a systematic error in the analysis of experimental data in Ref. [5], the calculation of $B(E2)$ and $B(M1)$ values is also performed with $e^{\mathrm{vib}} = 1.7$, and with maximal possible fermion gyromagnetic ratios: $g_l^\pi = 1.1$, $g_s^\pi = g_s^{\pi,\mathrm{free}} = 5.586$, $g_l^\nu = -0.1$, and $g_s^\nu = g_s^{\nu,\mathrm{free}} = -3.826$. The results are presented in Fig. 6, where the $B(E2)$ and $B(M1)$ values for interband transitions are presented, too. The strong experimental interband $E2$ transitions are a consequence of the mixing between the bands that for $I \geqslant 37/2$ are very close in energy. This mixing between the bands shifts some of the intraband strength to the interband one, which becomes strong. In IBFM, the partner bands remain separated and the significant mixing does not occur. Therefore, the intraband transitions remain large, while the interband transitions remain small.

Details of the structure of the yrast and yrare states based on the $\nu h_{11/2}(\pi h_{11/2})^2$ configuration depend on the strengths
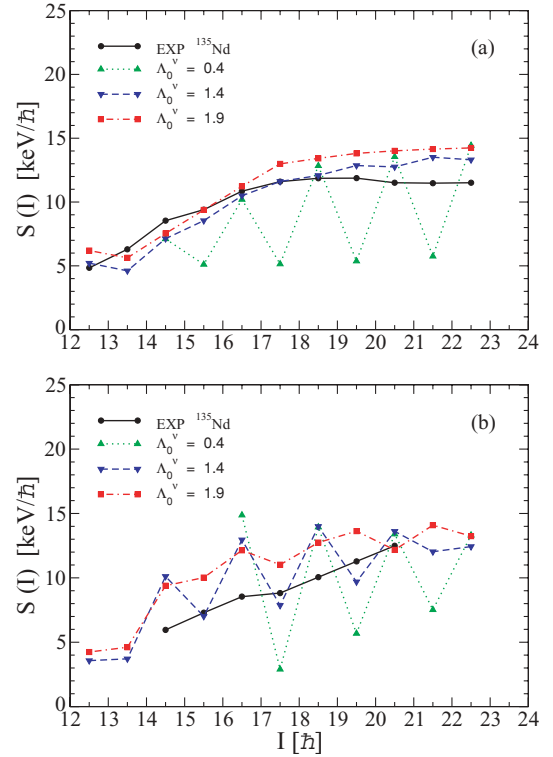

FIG. 7. (Color online) Experimental and IBFM signature $S(I) = [E(I) - E(I-1)]/2I$ vs spin plots for different strengths Λ_0^ν (in MeV) for the (a) yrast band A and (b) yrare band B in ^{135}Nd.

of several boson-fermion and fermion-fermion interactions, but the general pattern depends almost exclusively on the strength of the boson-fermion exchange interaction for odd neutrons Λ_0^ν. For $\Lambda_0^\nu \approx 0$ MeV, the bandhead of the yrast band is $31/2$. In this band, the branch of unfavored states $33/2, 37/2, 41/2$ is close in excitation energy to the branch of favored states $35/2, 39/2, 43/2$. Therefore, the band consists of closely lying doublets of states $(33/2, 35/2)$, $(37/2, 39/2)$, $(41/2, 43/2)$, etc. Increasing Λ_0^ν, the spin of the bandhead is shifted to lower spin values, while the yrast band gradually loses the doublet structure; and for $\Lambda_0^\nu = 1.4$ MeV, the value adopted for band GS, it becomes a rotational-like $\Delta I = 1$ band. The excitation energy vs spin dependence is very similar to the one in band A. For stronger Λ_0^ν this behavior is preserved. The signature $S(I) = [E(I) - E(I-1)]/2I$ vs spin plots for different strengths Λ_0^ν are presented in Fig. 7. For $\Lambda_0^\nu = 1.9$ MeV, the signature $S(I)$, for $I \geqslant 37/2$, loses the staggering and attains a smooth behavior almost without a spin dependence, indicating the change from the planar to the chiral regime. The calculated slope in the chiral regime is slightly steeper than the experimental one. Evidently, the IBM-1 triaxial equilibrium minimum is somewhat broader and the shape fluctuations larger than they should be in ^{135}Nd. For a weak exchange interaction, $B(M1)$ values for transition deexciting states of the favored $35/2, 39/2, 43/2$ branch are far bigger than $B(M1)$ values for transition deexciting states of the unfavored $33/2, 37/2, 41/2$ branch. The staggering is washed out for $\Lambda_0^\nu \approx 1.4$ MeV. The $B(E2)$ values in the yrast band also display the staggering in phase with the staggering

of the $B(M1)$ values. It is washed out at the same exchange strength for which the $B(M1)$ staggering disappears.

The doublet structure of the yrare band is more pronounced than the doublet structure of the yrast band, and the change into the regular $\Delta I = 1$ type is slower than in the yrast band. It reaches the rotational-like regularity for $\Lambda_0^\nu \approx 1.9$ MeV. The $B(M1)$ values for transitions deexciting all yrare states are almost zero for a weak exchange interaction. For a stronger exchange interaction, the pattern changes to a staggering in phase with the staggering in the yrast band. The staggering is washed out for $\Lambda_0^\nu \approx 1.9$ MeV. As in the yrast band, in the yrare band the $B(E2)$ values display the same staggering that consistently is washed out for the same exchange strength for which the $B(M1)$ staggering is washed out, too. The fact that for a wide range of weak and moderate strengths of the exchange interaction for odd neutrons the yrare "band" consists of $E2$ transitions only, means that in that regime it in fact consists of two $\Delta I = 2$ bands. The transformation of these bands in a rotational-like $\Delta I = 1$ band is due to the exchange interaction, i.e., to the antisymmetrization of odd neutrons with the neutron structure of the bosons.

IV. $N = 77$ NUCLEI

A negative-parity three-quasiparticle yrast band, with transition energies similar to the ones in band A, was observed in ^{137}Nd [24] and ^{139}Sm [22]. In Refs. [22,24] it was interpreted as the $(\nu h_{11/2})^3$ band. In ^{137}Nd, the $\nu h_{11/2}(\pi h_{11/2})^2$ configuration has been assigned to the yrare band with a bandhead 31/2. The question arises as to whether the two twin bands in ^{137}Nd can be interpreted as chiral partner bands. We have therefore performed calculations also for ^{137}Nd to investigate to what extent the three-quasiparticle twin bands have a chiral character.

The IBFM approach in the cases of ^{135}Nd, ^{137}Nd, and ^{139}Sm basically differs only in the strength Λ_0^ν of the boson-fermion exchange interaction for odd neutrons. In ^{135}Nd, Λ_0^ν is big, while in ^{137}Nd and ^{139}Sm, $\Lambda_0^\nu = 0$ MeV. The theoretical results for ^{137}Nd and ^{139}Sm would be the same as in Refs. [22,24] for any reasonably small value of Λ_0^ν. From the microscopic ground, the strength Λ_0^ν decreases when approaching the closed shell. For negative-parity states, the contribution of $\nu h_{11/2}$ neutrons, in the internal structure of bosons, is important. Although, the IBM-1/IBFM-1 models do not distinguish between proton bosons and neutron bosons, the number of bosons for ^{135}Nd, ^{137}Nd, and ^{139}Sm that are due to neutrons is half the number of valence neutron holes with respect to the $N = 82$ shell closure. In ^{135}Nd, three bosons are made of neutron holes, while in ^{137}Nd and ^{139}Sm there are only two. The contribution of the antisymmetrization of odd neutrons with the neutron structure of bosons, i.e., Λ_0^ν, is therefore smaller in ^{137}Nd and ^{139}Sm than in ^{135}Nd. The exchange interaction is also reduced in ^{137}Nd and ^{139}Sm, being the two nuclei less deformed, and therefore the $\nu h_{11/2}$ subshell is less spread out in energy in a Nilsson-like diagram. The contribution of the exchange interaction in ^{137}Nd and ^{139}Sm is further reduced by a bigger occupation probability of the $\nu h_{11/2}$ configuration. The structure of band G in ^{137}Nd and
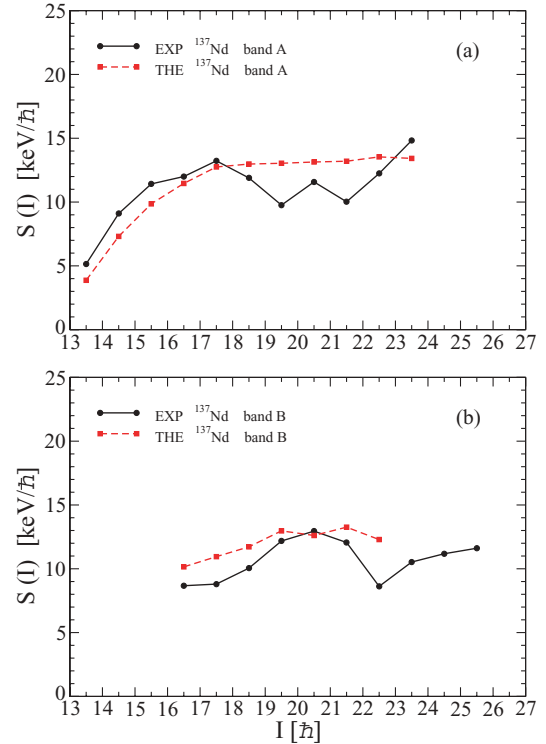

FIG. 8. (Color online) Experimental and IBFM signature $S(I) = [E(I) - E(I-1)]/2I$ vs spin plots for the (a) yrast band A and (b) yrare band B in ^{137}Nd.

^{139}Sm reflects the absence of the contribution of the exchange interaction: the lowest state is 11/2 and the higher states form doublets of more or less closely lying states. All these arguments lead to the conclusion that in ^{137}Nd and ^{139}Sm, a pair of twin bands analogous to those in ^{135}Nd will not appear.

In Ref. [24], it has been shown that the staggering in the ground-state band and the nonstaggered three-quasiparticle bands 6 and 7 of ^{137}Nd can be qualitatively, but not quantitatively, reproduced by the shape change induced by the polarizing effects of the quasiparticles from broken pairs. The lack of staggering in the three-quasiparticle bands 6 and 7 of ^{137}Nd could not be well reproduced by an increase of the neutron dynamical interaction, the only one that could be invoked in the attempt to take into account the polarizing effects of the quasiparticles from the broken pairs. In ^{135}Nd, the shape change between the ground-state band and the three-quasiparticle bands is small and can be ignored. The only interaction that can reproduce the nonstaggered behavior of both the ground-state and the three-quasiparticle bands is the exchange interaction.

The calculation for ^{135}Nd shows that the strength of the boson-fermion exchange interaction for odd neutrons is stronger for $\nu h_{11/2}(\pi h_{11/2})^2$ structures than for states of band G based on $\nu h_{11/2}$. The difference is sizable but not as drastic as it would be if the same effect were present in ^{137}Nd and ^{139}Sm nuclei. Nevertheless, different driving forces for $h_{11/2}$ neutrons and protons in a γ-soft potential make the possibility of finding the partner band of the yrast band [and the assignation of $\nu h_{11/2}(\pi h_{11/2})^2$ structure to both of them]
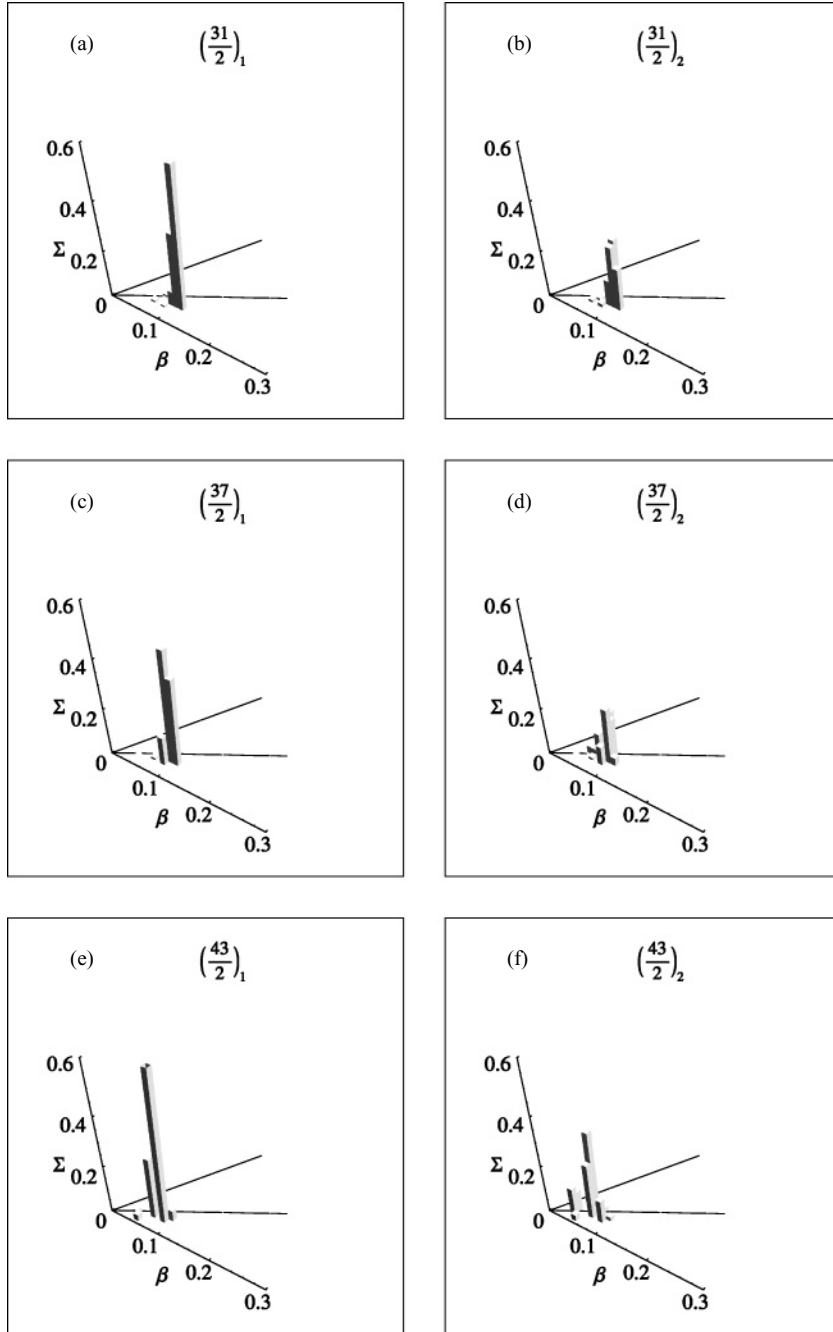
FIG. 9. IBFM β and γ distributions in ^{137}Nd, defined as in Ref. [13], for the (a) $31/2_1$ and (b) $31/2_2$ states; the (c) $37/2_1$ and (d) $37/2_2$ states; and the (e) $43/2_1$ and (f) $43/2_2$ states. The axes in the β-γ plane have $\gamma = 0°$ and $\gamma = 60°$, while the middle line in the β-γ plane marks $\gamma = 30°$.

in ^{137}Nd not very likely, but still possible. It could be that the same exchange interaction is the main mechanism responsible for the increased regularity of the three-quasiparticle bands also in ^{137}Nd, and the effect observed in ^{135}Nd is present in all nuclei around ^{135}Nd at high spins. The measurement of $B(E2)$ and $B(M1)$ values in ^{137}Nd can give a better insight into the microscopic mechanism responsible for the formation of chiral structures in nuclei.

To test such a possibility, we have performed IBFM calculations for ^{137}Nd, following the same line as in the ^{135}Nd case. For the core nucleus ^{138}Nd, we take the set of parameters for the IBM-1 boson Hamiltonian (all values

in MeV): $\epsilon = 0.24$, $V_0 = -0.3$, $V_2 = 0.0$, $C_0 = 0.2$, $C_2 = 0.036$, $C_4 = 0.187$, the number of bosons $N = 7$, and $\Theta_3 = 0.01$ MeV. This parametrization gives the structure of ^{138}Nd that slightly differs from the one in Ref. [24] in the same way as the parametrization for ^{136}Nd in the present article differs from the one in Ref. [25]. For the proton quasi-particle energies, occupation probabilities, boson-fermion interaction strengths for protons Γ_0^π, Λ_0^π, A_0^π, the parameter η in the quadrupole operator, the proton pair-breaking interaction U_2, and the strength of the residual interaction between unpaired protons $V_{\delta\pi\pi'}$, we take the same values as in the calculation for ^{135}Nd. For protons, the only difference is in

the value χ in the quadrupole operator of the dynamical interaction. We take $\chi = -0.1$, which is consistent with the change of the sign of χ at $N = 78$. From the BCS calculation with neutron single-particle energies from Refs. [22,24] for the $N = 50$–82 shell and from this article for the $N = 82$–126 shell (0.05, 0.71, 2.24, 2.81, 1.75, 7.60, 9.30, and 9.40 MeV, for $\nu d_{5/2}$, $\nu g_{7/2}$, $\nu s_{1/2}$, $\nu d_{3/2}$, $\nu h_{11/2}$, $\nu f_{7/2}$, $\nu p_{3/2}$, and $\nu h_{9/2}$), with the pairing strength $G = 26/A$ MeV, we take the neutron quasiparticle energies and occupation probabilities: $\varepsilon(\nu h_{11/2}) = 1.63$ MeV, $\varepsilon(\nu f_{7/2}) = 4.91$ MeV, $\varepsilon(\nu p_{3/2}) = 6.57$ MeV, $\upsilon^2(\nu h_{11/2}) = 0.84$, $\upsilon^2(\nu f_{7/2}) = 0.02$, and $\upsilon^2(\nu p_{3/2}) = 0.01$. For the boson-fermion interaction strengths for neutrons, in the space of one-quasiparticle configurations, we take the values from Ref. [24]: $\Gamma_0^\nu = 0.3$, $\Lambda_0^\nu = 0$, $A_0^\nu = 0$ (all values in MeV). The parameters $\chi = -0.6$ and $\eta = -0.35$ in the quadrupole operator of the dynamical boson-fermion interaction for odd neutrons are the same as in the calculation for ^{135}Nd. The residual proton-neutron interaction does not influence the structure of possible twin bands (due to their high spins) but shifts their excitation energies with respect to the ground-state band. In this case, it is taken as the volume δ-interaction $V_{\pi\nu} = 4\pi\, V_\delta\, \delta(\mathbf{r}_\pi - \mathbf{r}_\nu)$ with the strength $V_\delta = -70.0$ MeV.

The adopted set of IBFM parameters is consistent with parametrizations of ^{137}Nd neighbors. Reasonable changes of these parameters do not change the structure of possible high-spin $\nu h_{11/2}(\pi h_{11/2})^2$ twin bands. It depends mainly on the boson-fermion interaction strengths for neutrons in the space of three-quasiparticle configurations. A structure, closest to the observed, is obtained for $\Gamma_0^\nu = 0.4$, $\Lambda_0^\nu = 1.0$, and $A_0^\nu = 0.08$ (all values in MeV). These values are similar to those in ^{135}Nd, with Λ_0^ν, as expected, being smaller. In the calculation of $B(E2)$ and $B(M1)$ values, we use the effective charges and gyromagnetic ratios: $e^\pi = 1.0$, $e^\nu = 0.5$, $e^{\mathrm{vib}} = 1.0$, $\chi = -0.35$, $\eta = -0.35$, $g_l^\pi = 1$, $g_s^\pi = 0.9 g_s^{\pi,\mathrm{free}} = 5.027$, $g_l^\nu = 0$, $g_s^\nu = 0.3 g_s^{\nu,\mathrm{free}} = -1.148$, and $g_R = 0.2$. The calculations have shown that in this case the possible choices of effective charges and gyromagnetic ratios strongly influence the magnitude of $B(E2)$ and $B(M1)$ values, but do not change significantly the slopes of the $B(E2)$ vs spin and $B(M1)$ vs spin curves or the relative relations of $B(E2)$ and $B(M1)$ values of transitions in bands A and B. We notice that χ in the $E2$ operator, as well as in the quadrupole operator for the effective deformation, is the mean value of the proton and neutron χ.

The comparison of calculated and observed twin bands in ^{137}Nd is not simple, because both bands are crossed by other bands in the region of interest, band A at spin 37/2 and band B at spin 43/2. In the signature $S(I) = [E(I) - E(I - 1)]/2I$ vs spin plot (Fig. 8), we present the signature up to the highest observed state (after the crossing). The theoretical values would correspond to ideal bands in ^{137}Nd that are not crossed by other, probably four-quasiparticle, bands. Because of the truncation of the boson basis, the calculated band B is presented up to spin 45/2. The calculated staggering in both bands attains a smooth behavior almost without a spin dependence, indicating that the chiral interpretation is not excluded. The comparisons of the calculated ζ, ψ, ξ, and σ distributions for the $I = 39/2$ yrast and yrare states in
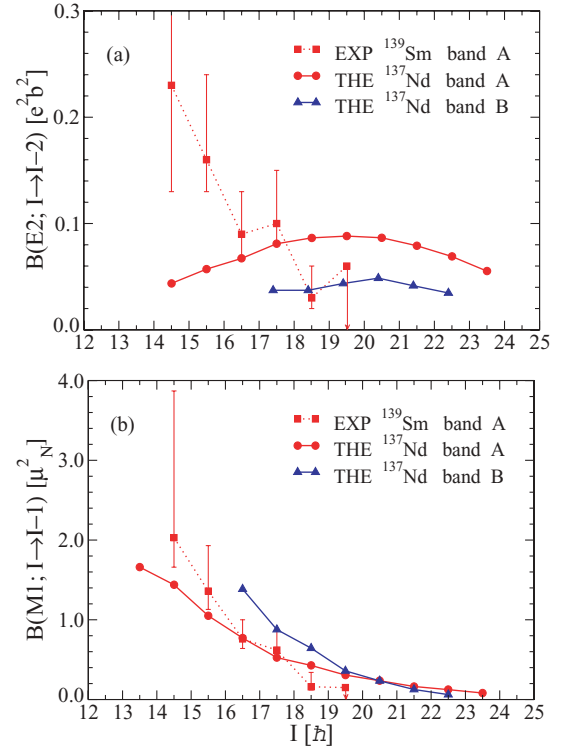

FIG. 10. (Color online) Calculated (THE) $B(E2)$ and $B(M1)$ values for transitions in the yrast band A and side band B in ^{137}Nd. (a) $B(E2)$ values. (b) $B(M1)$ values for $\Delta I = 1$ transitions. For comparison, the experimental (EXP) values in ^{139}Sm are also shown.

^{137}Nd, with the distributions in ^{135}Nd (Figs. 3 and 4), also show no significant differences. The yrare states show more axial components, but still far less than in ^{134}Pr, leaving the chiral interpretation possible. The distributions of β and γ deformation parameters (Fig. 9) make the chiral interpretation questionable. Shape fluctuations in band B are far more pronounced than in band A. The fluctuations are not reduced for higher spins. On the contrary, in band B the shape fluctuations are enhanced for higher spins, and besides triaxial slightly prolate components, oblate components appear in the distribution. As IBM/IBFM in the version with one type of bosons cannot generate very realistic triaxial minima, it is reasonable to expect that a more realistic potential would generate more oblate components in band B at lower spins, leading to the conclusion that in $N = 77$ nuclei the structure of twin bands is more determined by shape fluctuations and prolate-oblate coexistence than by chirality. Preliminary results on the $N = 77$ ^{135}Ce nucleus show the existence of a twin band structure similar to that in ^{137}Nd [26]. The fact that in ^{135}Ce, states of band B are lower in excitation energy than the corresponding states of the same spin in band A, even at relatively low spin, could be an argument in favor of this conclusion.

The calculated $B(E2)$ and $B(M1)$ values (Fig. 10) are compared with experimental data in ^{139}Sm, the only $N = 77$ nucleus for which data is available [27]. The calculated $B(M1)$

vs spin curve is steeper than for ^{135}Nd, with $B(M1)$ values being bigger in band B than in band A at moderate spins. A steep decrease of $B(M1)$ values is observed in ^{139}Sm, and preliminary data for ^{135}Ce [26] indicate that $B(M1)$ values for interband transition deexciting states in band B are rather big at moderate spins. The calculated $B(E2)$ values are by a factor of 2 bigger in band A than in band B, in agreement with results of the analysis of shape fluctuations that point to different deformations in the partner bands. Preliminary data for ^{135}Ce [26] indicate small $B(E2)$ values in band B. The calculated values are consistent with experimental data in ^{137}Nd [24] and ^{139}Sm [22], where $E2$ transitions have not been observed in band B.

A strong exchange interaction is not the characteristic of only a certain type of nuclei. It is important in deformed, transitional, and spherical nuclei. In axially deformed nuclei, it can be the dominant part of the boson-fermion interaction. The fact that it could be strong in such nuclei as ^{137}Nd and ^{139}Sm points to the possible strong correlation between the exchange interaction and the triaxiality. Intuitively, the triaxiality brings the orbitals split away by the quadrupole deformation closer and favors the exchange between the odd neutron and the rest of the valence neutrons. Since these nuclei are not rigid but γ-soft, the coupling of odd fermions to shape degrees of freedom is the dominant mechanism, leading to a chirality of dynamical origin. In odd-mass nuclei, the conditions for chirality are more favorable than in odd-odd, because the two-particle angular momentum is longer than the one-particle angular momentum in odd-odd nuclei. When the exchange interaction is too strong, the soft potential allows the coupling of odd fermions to other higher lying core structures, increasing the shape fluctuations. The deformation of the two partner bands is different, most of the signatures of chirality are washed away, and the vicinity of the excitation energies of the two bands remains the only fingerprint of chirality.

V. CONCLUSIONS

Theoretical investigation of the ^{135}Nd nucleus in the framework of the interacting boson-fermion model has shown that a pair of three-quasiparticle bands can be interpreted as twin chiral bands based on the $\nu h_{11/2}(\pi h_{11/2})^2$ configuration, as was recently shown in the TAC/RPA approach [5]. The formation of the chiral pattern, in this odd-A nucleus with a γ-soft core, is possible in IBFM, however, only if the boson-fermion exchange interaction is strong. Since the occupation probability of the odd proton $\upsilon^2(\pi h_{11/2}) = 0.09$ is very low, the effect of the boson-fermion exchange interaction for the odd proton is small. But the occupation probability $\upsilon^2(\nu h_{11/2}) = 0.62$ for the odd neutron is of the order where the effect of the boson-fermion exchange interaction for the odd neutron is maximal. Calculations show that this interaction, which is a result of the antisymmetrization of odd neutrons with the neutron structure of the bosons, plays the dominant role in the formation of the chiral pattern. The experimentally observed decay properties of the chiral-candidate bands can be theoretically reproduced only when the strength of the exchange interaction for odd neutrons is strong but limited to a certain interval. The strength of the interaction for three-quasiparticle chiral states has to be stronger than for one-quasiparticle states. The theoretical investigation of ^{137}Nd within IBFM reveals the rather reduced chiral character of the twin bands, which can have a structure determined by shape fluctuations and prolate-oblate coexistence. The dominant role of the exchange interaction, i.e., of the antisymmetrization of odd fermions with the fermion structure of the bosons, in the formation of different types of chiral patterns has also been observed in odd-odd nuclei [20]. The mechanism that, in the IBFM/IBFFM framework, connects chirality and the Pauli principle is an open question, both on the microscopic and algebraic level. It is possible that is due to some symmetry.

[1] S. Frauendorf and J. Meng, Nucl. Phys. **A617**, 131 (1997).

[2] V. I. Dimitrov, S. Frauendorf, and F. Dönau, Phys. Rev. Lett. **84**, 5732 (2000).

[3] K. Starosta, T. Koike, C. J. Chiara, D. B. Fossan, and D. R. LaFosse, Nucl. Phys. **A682**, 375c (2001).

[4] S. Zhu *et al.*, Phys. Rev. Lett. **91**, 132501 (2003).

[5] S. Mukhopadhyay *et al.*, Phys. Rev. Lett. **99**, 172501 (2007).

[6] D. Vretenar, G. Bonsignori, and M. Savoia, Z. Phys. A **351**, 289 (1995).

[7] I. Ragnarsson and P. Semmes, Hyperfine Interact. **43**, 423 (1988).

[8] K. Starosta, C. J. Chiara, D. B. Fossan, T. Koike, T. T. S. Kuo, D. R. LaFosse, S. G. Rohoziński, Ch. Droste, T. Morek, and J. Srebrny, Phys. Rev. C **65**, 044328 (2002).

[9] S. Brant, V. Paar, and D. Vretenar, Z. Phys. A **319**, 355 (1984).

[10] S. Brant and V. Paar, Z. Phys. A **329**, 151 (1988).

[11] S. Brant, D. Vretenar, and A. Ventura, Phys. Rev. C **69**, 017304 (2004).

[12] D. Tonev *et al.*, Phys. Rev. Lett. **96**, 052501 (2006).

[13] D. Tonev *et al.*, Phys. Rev. C **76**, 044313 (2007).

[14] F. Iachello and A. Arima, *The Interacting Boson Model* (Cambridge University Press, Cambridge, England, 1987).

[15] A. Arima and F. Iachello, Phys. Rev. Lett. **35**, 1069 (1975); Ann. Phys. (NY) **99**, 253 (1976); **111**, 201 (1978); **123**, 468 (1979).

[16] F. Iachello and O. Scholten, Phys. Rev. Lett. **43**, 679 (1979).

[17] F. Iachello and P. Van Isacker, *The Interacting Boson Fermion Model* (Cambridge University Press, Cambridge, England, 1991).

[18] K. Heyde, P. Van Isacker, M. Waroquier, and J. Moreau, Phys. Rev. C **29**, 1420 (1984).

[19] R. F. Casten, P. von Brentano, K. Heyde, P. Van Isacker, and J. Jolie, Nucl. Phys. **A439**, 289 (1985).

[20] S. Brant, D. Tonev, G. de Angelis, and A. Ventura, Phys. Rev. C **78**, 034301 (2008).

[21] F. Iachello and D. Vretenar, Phys. Rev. C **43**, R945 (1991).

[22] C. Rossi Alvarez *et al.*, Phys. Rev. C **54**, 57 (1996).

[23] G. de Angelis *et al.*, Phys. Rev. C **49**, 2990 (1994).

[24] C. M. Petrache *et al.*, Nucl. Phys. **A617**, 228 (1997).

[25] D. Vretenar, S. Brant, G. Bonsignori, L. Corradini, and C. M. Petrache, Phys. Rev. C **57**, 675 (1998).

[26] R. Palit (private communication).

[27] A. A. Pasternak, Eur. Phys. J. A **37**, 279 (2008).